Available online at www.sciencedirect.com
SCIENCE DIRECT®
Journal of Process Control 15 (2005) 771–784
JOURNAL OF PROCESS CONTROL
www.elsevier.com/locate/jprocont

Boundary control for an industrial under-actuated tubular chemical reactor

D. Del Vecchio [a], N. Petit [b,*]

[a] Control and Dynamical Systems, California Institute of Technology, Mail Code 107-8l, 1200 E California Blvd. Pasadena, CA 91125, USA
[b] Centre Automatique et Systèmes, Ecole Nationale Supérieure des Mines de Paris, 60, boulevard Saint-Michel, 75272 Paris Cedex 06, France

Received 8 March 2004; received in revised form 28 February 2005; accepted 11 March 2005

Abstract

Several control strategies are presented and studied for an industrial under-actuated tubular chemical reactor. This work presents a case-study of the performance of a decentralized versus centralized control strategy. The tubular reactor under consideration is characterized by nonlinear kinetic laws, and it has some structural constraints on the location of the heat exchangers and of the sensors. For this system, a set of PI controllers is considered and a multivariable LQR controller is constructed to optimally choose the gains. The performance of these control strategies is studied. Finally, a direct numerical treatment of optimal control of the partial differential equations is presented. Industrial results are given for the linear controllers. Simulations emphasize the possible relevance of a direct numerical treatment of the nonlinear partial differential equations.

Keywords: Polystyrene; Tubular reactor; Control; Optimization; Industrial application

1. Introduction

The contribution of this paper is a study of different control strategies for a class of tubular reactors. The application underlying this study is a reactor in the ATOFINA PS (polystyrene) plant in Carling, France. We present a model of the tubular reactor used in this plant, which is characterized by nonlinear kinetic laws and by an under-actuated structure due to the choice of heat exchangers and sensor locations.

Around a steady production state (corresponding to an average of 120 kT/year), the grade of the polystyrene produced in this plant critically depends on the temperature profile along the reactor. In fact, the real control objective is temperature control. Other controlled variables such as molecular mass distribution are controlled using other inputs such as dilution. This is different from other reactors (see e.g. [1] for a survey of polymerization reactor control) where monomer conversion is usually considered as a critical value. In this plant, quality constraints (in connection to further injection and thermoforming applications) are tight and they directly translate to temperature constraints.

The grade of the produced polymer is scheduled with respect to economical considerations. This induces frequent changes in the setpoints that have to be precisely and quickly met to optimize profit and minimize off-spec products.

This paper proposes several control schemes to improve upon the results obtained with the existing PI controllers used in the plant. In particular, for a decentralized PI scheme, we show that the choice of the measurement and setpoints affects both transient and asymptotic performance. Then, a centralized PI scheme

* Corresponding author. Tel.: +33 1 4051 9330; fax: +33 1 4051 9165.
E-mail address: nicolas.petit@ensmp.fr (N. Petit).

0959-1524/$ - see front matter © 2005 Elsevier Ltd. All rights reserved.
doi:10.1016/j.jprocont.2005.03.004

is proposed, where the proportional gains are designed using an LQR design. This approach can be considered as a weighting of the input of a PI controller based on the model structure. Finally, a nonlinear centralized controller is proposed and its performance compared with the others. This work relies on the controller upgrade project that was carried out at the ATOFINA plant by a joint team of TOTAL engineers and researchers from École des Mines de Paris, which is reported in [2].

We propose three different control strategies ranging from fully decentralized to fully centralized. This work can be seen as an industrial scale case-study of the role of a decentralized versus centralized control strategy. This question was raised by several authors in various fields of the process industry [3–5], and we found it particularly relevant in this problem. From our point of view and from this particular study, we believe it needs to be answered with two facts on mind: performance requirements and availability of efficient numerical tools and accurate models.

This paper considers the problems as they appeared when trying to improve the existing PI controllers. In Section 2, we give the model of the plant. In Section 3, we underline the importance of the right choice of PI structure for performance improvement. In Section 4, we explain the design and tuning of an LQR controller that has been successful since when it was installed in 2000 (overall load was increased by more than 10%). Industrial results are given. Finally in Section 5, we propose an approach based on the direct treatment of the nonlinear partial differential equations that govern the system. This approach relies on the NTG optimal control software package designed for PDEs [6,7]. We compare the results of different control strategies and show that this last method, when a good knowledge of the process dynamics is available, is efficient and flexible.

2. Model of the reactor

The process under study is a polymerization tubular exothermic reactor with heat exchangers on the sides and with plug flow, see Fig. 1.

The styrene monomer enters the tubular reactor at a constant temperature at point I (see Fig. 1) along with the peroxide initiator. The monomer reacts inside the tubular reactor as it travels to point O. The tubular reactor is equipped with heat exchangers to evacuate the reaction exothermicity.

This tubular reactor is frequently subject to strong oscillations. These are usually interpreted as temperature perturbations propagating through the system (these perturbations can arise from various phenomena: in [8] it is shown that for such tubular reactors, jacket temperature perturbations may lead to oscillatory dynamic responses[1]).

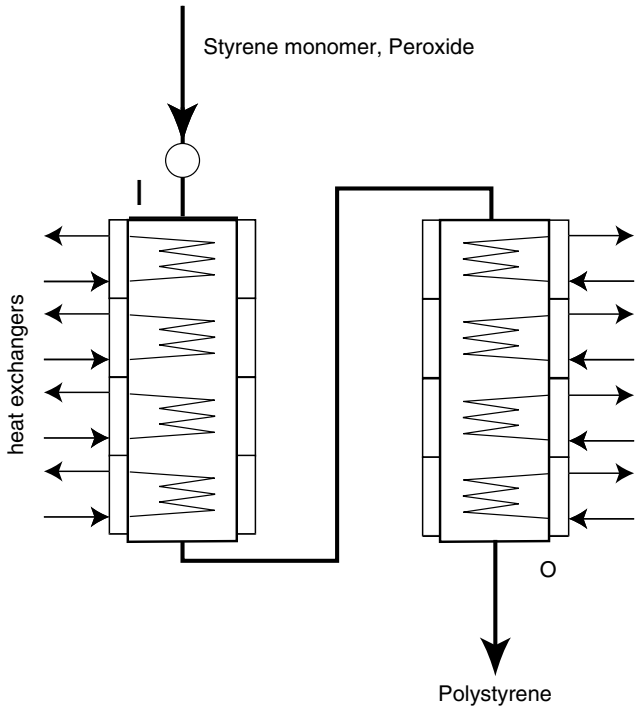

Fig. 1. Schematic of the tubular reactor.

2.1. Under-actuated structure

A close-up view of the reactor shows the heat exchangers and the temperature sensors (see Fig. 2). The reactor is divided in eight zones, each of which has two sensors and one heat exchanger. One is located at the middle of the zone, and one is located at its end. More complicated sensor configurations (with variable number of sensors and varying locations) could also be considered but these are out of the scope of this paper (optimal placement for such process is indeed an important topic as underlined in [9]). In this study, the total length of the tubular reactor is scaled to 1, and the velocity v of the flow inside the reactor is 0.01. This system can be considered as under-actuated since the eight heat exchangers can only produce piecewise constant control along the reactor's length. Classically, polymer viscosity is very high and laminar flow is assumed for modelling. The industrial tubular reactor underlying this study is very thin due to the heat transfer constraints. These factors lead us to model the reactor dynamics as a set of one-dimensional partial differential equations (PDE). Measurements of the temperature T are available at a

[1] Interested readers can also find in the previous reference developments of a model predictive control that allows the successful control of monomer conversion in a different context.

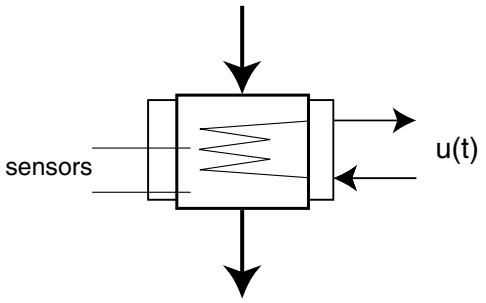

Fig. 2. Close-up view of the reactor.

finite number of locations along the reactor. Online measurement of monomer conversion x and peroxide concentration G is currently out of reach.

2.2. Model

Let $t \in \mathbb{R}^+$ represent the time and $z \in [0,1]$ the coordinate along the reactor, then the dynamics of the tubular reactor can be described by a set of three partial differential equations

$$\begin{cases} C_p(T,x)\left(\dfrac{\partial T(t,z)}{\partial t} + v\dfrac{\partial T(t,z)}{\partial z}\right) = \Delta H(T) r(T,x,G) + u, \\ \dfrac{\partial x(t,z)}{\partial t} + v\dfrac{\partial x(t,z)}{\partial z} = r(T,x,G), \\ \dfrac{\partial \log(G(t,z))}{\partial t} + v\dfrac{\partial \log(G(t,z))}{\partial z} = f(T), \end{cases} \tag{1}$$

with boundary and initial conditions

$$T(t,0) = T_{t,0}, \quad x(t,0) = x_{t,0}, \quad G(t,0) = G_{t,0}, \tag{2}$$

$$T(0,z) = T_{ic}(z), \quad x(0,z) = x_{ic}(z), \quad G(0,z) = G_{ic}(z) \tag{3}$$

where notation is defined in Table 1. The terms on the right hand side of (1) are as follows. We have

$$\Delta H(T) = a_0 + \frac{a_1}{T+273} + a_2(T+273),$$

$$r(T,x,G) = k_1(T,x,G)k_2(T,x),$$

Table 1
Nomenclature

Symbols	Quantity	Unit
$T(t,z)$	Temperature in the reactor	Celsius degrees
$x(t,z)$	Monomer conversion	–
$G(t,z)$	Peroxide concentration	$\mathrm{mol\,m^{-3}}$
v	Velocity of the particles along the reactor	$\mathrm{m\,s^{-1}}$
$C_p(T,x)$	Heat capacitance of the fluid	$\mathrm{J\,K^{-1}}$
$u(t,z)$	Heat exchange (control)	$\mathrm{J\,s^{-1}}$
$r(T,x,G)$	Rate of reaction	$\mathrm{s^{-1}}$
$\Delta H(T)$	Reaction enthalpy	K

where a_0, a_1 and a_2 are constant coefficients and k_1 is of the form

$$k_1(T,x,G) = \sqrt{F_1(T,x) + GF_2(T,x)}, \tag{4}$$

with F_1 and F_2 two smooth functions, while

$$f(T) = e_0 \exp\left(\frac{e_1}{T+273}\right),$$

where e_0 and e_1 are constant coefficients. A polynomial fit is used for $C_p(T,x)$ (affine function in x with third order polynomial in T as coefficients). This kinetic model arises from the classic Hui and Hamielec approach [10]. Typical values of the $r(T,x,G)\Delta H$ term are shown in Fig. 3 (where scales are omitted for confidentiality reasons). One clearly sees that the reaction mostly takes place in the middle of the tubular reactor.

The first equation in (1) is a heat balance, the second describes the conversion of monomer, and the third one represents the organic peroxide initiator dynamics that is thermally activated. Details about the kinetic scheme of this polymerization reaction and the role of the peroxide initiator can be found in [11]. The velocity v is considered constant. We thus neglect the effect of density variations.

2.3. Control objectives

Two control problems are considered. In the first place, the problem of regulating the temperature profile along the reactor to a given profile T_{sp} is considered, which guarantees good product quality at the end of the reactor. Then, we consider the problem of allowing fast transitions between desired temperature profiles corresponding to good product quality of different materials.

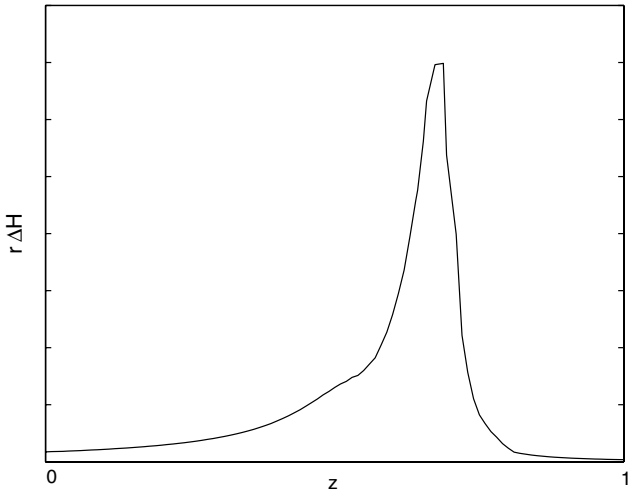

Fig. 3. Exothermicity along the reactor at steady state. Exact scales are omitted for confidentiality reasons.

2.4. Simulation setup

In this section, the testbed we base all our study on is considered. The three PDEs in Eq. (1) are discretized along the z variable to obtain three systems of ordinary differential equations (following the tanks-in-series model [12]). This approach is alike other methods found in the literature. Our model does not imply parabolic PDEs (i.e. with spatial diffusion operators) and so is not easily described by small finite-dimensional systems. In [13], a discretization of the coupled temperature and conversion PDEs similar to ours is used, but a different control structure is considered (control of temperature and concentration is achieved from the inlet side of the reactor). Radial variations are not taken into account either. Advanced methods could also be considered but are out of the scope of this study: e.g. in [14] a very fine representation of the model reactor (considering radial variation of all variables) is solved by the method of lines using either finite volume discretization or global spline orthogonal collocation.

Spatial discretization. The partial derivatives with respect to z are discretized using finite backward differences according to

$$\left.\frac{\partial W(t,z)}{\partial z}\right|_{(t,z_i)} \cong \frac{W(t,z_i)-W(t,z_{i-1})}{\delta_z},$$

for any variable of time and space W, where $(z_1,\ldots,z_n)$ are the cells, equally distributed in space, in which we discretize the reactor, and $\delta_z=(z_i-z_{i-1})$. As a result, letting $T_i(t)=T(t,z_i)$, $x_i(t)=x(t,z_i)$, $G_i(t)=G(t,z_i)$, $r_i=\Delta H(T_i)r(T_i,x_i,G_i)$, $k_i=r(T_i,x_i,G_i)$, $f_i=f(T_i)$, $C_{p,i}=C_p(T_i,x_i)$, we obtain the three systems of ordinary differential equations

$$\begin{cases}\dot{T}=AT+bc_T+C_p^{-1}(r+Bu),\\ \dot{x}=Ax+bc_x+k,\\ \dfrac{\mathrm{d}\log G}{\mathrm{d}t}=A\log G+bc_G+f,\end{cases} \tag{5}$$

where $T=(T_1,\ldots,T_n)^{\mathrm{T}}$, $x=(x_1,\ldots,x_n)^{\mathrm{T}}$, $G=(G_1,\ldots,G_n)^{\mathrm{T}}$, $r=(r_1,\ldots,r_n)^{\mathrm{T}}$, $k=(k_1,\ldots,k_n)^{\mathrm{T}}$, $f=(f_1,\ldots,f_n)^{\mathrm{T}}$, $bc_T=(T_{t,0},0,\ldots,0)^{\mathrm{T}}$, $bc_x=(x_{t,0},0,\ldots,0)^{\mathrm{T}}$, $bc_G=(\log(G_{t,0}),0,\ldots,0)^{\mathrm{T}}$, and C_p is a diagonal matrix with diagonal entries $C_{p,i}$. $A=\frac{v}{\delta_z}(a_{ij}=(-1)\delta_i^j+\delta_{i-1}^j)$ is the $n\times n$ backward differences matrix, B is the $n\times 8$ input matrix, and $u=(u_1,\ldots,u_8)^{\mathrm{T}}$. Each actuator i acts on its zone of competence, which will be referred to as zone i. In particular, if the ith zone has n_i cells, with $n_1+\cdots+n_8=n$, then in the ith column of B the first $n_1+\cdots+n_{i-1}$ elements are zeros, the elements from $n_1+\cdots+n_{i-1}+1$ to $n_1+\cdots+n_i$ are ones, and the remaining elements are zeros.

Other possible choices for the spatial discretization method include forward difference equations, centered difference equations and second order methods such as the Lax–Wendroff numerical scheme (see [15]). Forward difference approximation results into an unstable A matrix when $v>0$, which is our case. The centered difference approximation produces a matrix that has imaginary eigenvalues and therefore is not asymptotically stable. The Lax–Wendroff second order method produces a A matrix with complex eigenvalues causing unrealistic oscillations.

Simulation setup. The value of n is chosen to be 100. The reason of this choice is a compromise between the time needed for simulating the system and the accuracy to which the spatial partial derivative is approximated. The numerical damping induced on the transport phenomena drops by only 2% (using a standard Runge–Kutta solver) when n is increased from 100 to 200, while the required computational effort rises by 100%.

3. Basic PI control designs

Based on the model in (5), two PI schemes used in the industrial setting were considered. These are diagonal control structures. Classically, derivatives term (D) were omitted to prevent temperature sensor noise from being amplified. In these two schemes, only one measurement in each zone is used. In the first scheme, the measurement is taken at the center of the zone, while in the second scheme the measurement is taken at the end of the zone. From a theoretical point of view, these choices induce strong constraints on the controller structure and lead to performance deterioration when compared to the system with a full controller matrix (as pointed out in [16]). However, this deterioration has to be weighted against design simplicity and failure tolerance. In fact, each block controller can be designed for the isolated subsystem, and fewer controller parameters need to be chosen than for the full system. Further, stability and performance are preserved to some degree when individual sensors or actuators fail. This failure tolerance is an attractive feature in the industrial framework. Part of such a controller can be turned off without dramatically affecting the system.

3.1. PI controller with measurement at the center of the zone

In this context, only the eight sensors at the center of the zone are used. Let n_i be the number of cells in zone i, and let $T_{m_1},\ldots,T_{m_8}$ denote the measured temperatures, then we have that $m_i=\sum_{j=1}^{i-1}n_j+n_i/2$. Let $T_{\mathrm{sp}}=(T_{\mathrm{sp},1},\ldots,T_{\mathrm{sp},n})$ and $u_{\mathrm{ref}}=(u_{\mathrm{ref},1},\ldots,u_{\mathrm{ref},8})^{\mathrm{T}}$ denote the reference temperature profile and the corresponding

constant reference input respectively. The closed loop control laws are

$$u_i = -K_{\mathrm{P},i}(T_{m_i} - T_{\mathrm{sp},i}) - K_{\mathrm{I},i}\int (T_{m_i} - T_{\mathrm{sp},i}) + u_{\mathrm{ref},i},$$
$$i \in \{1,\ldots,8\}. \quad (6)$$

The gains $K_{\mathrm{P},i}$ and $K_{\mathrm{I},i}$ are tuned in descending cascade (we tune first the PI of the first zone, and then the PI of the following zones by leaving the already tuned PI on) by means of the Ziegler–Nichols closed loop PID tuning rule (see for example [17]). When a step disturbance of amplitude 10% is applied at the entrance of the reactor, the response of the closed loop system is given in Fig. 4. The left plot of the same figure shows the asymptotic temperature profile along the reactor. The performance at locations different from the ones at which the measurement occurs is not satisfactory: only the measured temperatures are well tracked. The right plot shows the control effort $u_i - u_{\mathrm{ref},i}$.

3.2. PI controller with measurement at the end of the zone

In this setup, only the eight end of zone temperature sensors $T_{m_1},\ldots,T_{m_8}$ are used. With n_i the number of cells in zone i, we have $m_i = \sum_{j=1}^{i} n_j$. The closed loop control law u is given again by expression (6), where the reference value $T_{\mathrm{sp},i}$ and $u_{\mathrm{sp},i}$ are appropriately computed. Proportional and integral gains are still tuned in descending cascade using Ziegler–Nichols method. Closed loop response are shown in Fig. 5.

By contrast with results in Fig. 4, this control design produces an asymptotic temperature profile that is satisfactory not only where the measurement is performed. An analysis of such a performance difference is explained in the following section.

3.3. Comparisons of the two measurement schemes

Spatially distributed offsets in the asymptotic temperature profile still persist when the integral part of the

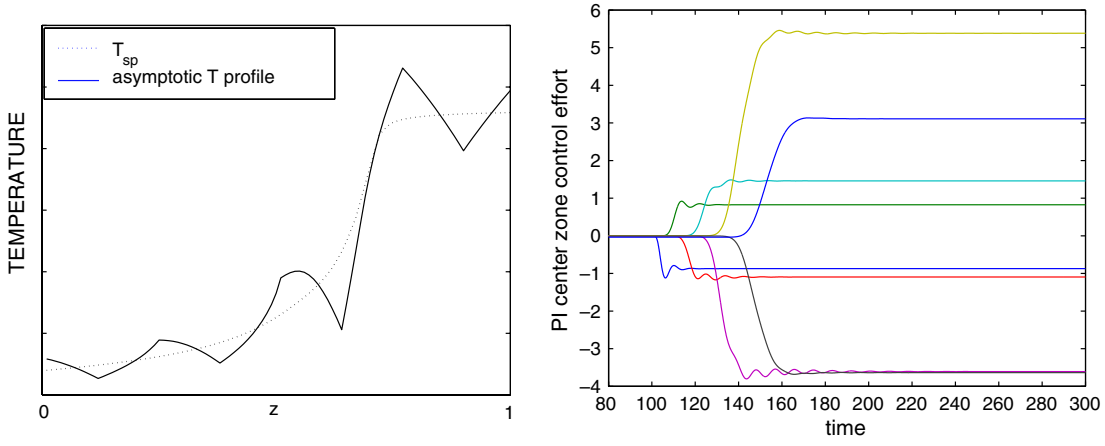

Fig. 4. PI controller with measurement at the center of the zone. Performance of the closed loop system when a step of amplitude 10% of input temperature is applied at the entrance of the reactor. Left: asymptotic temperature profile. Right: control effort.

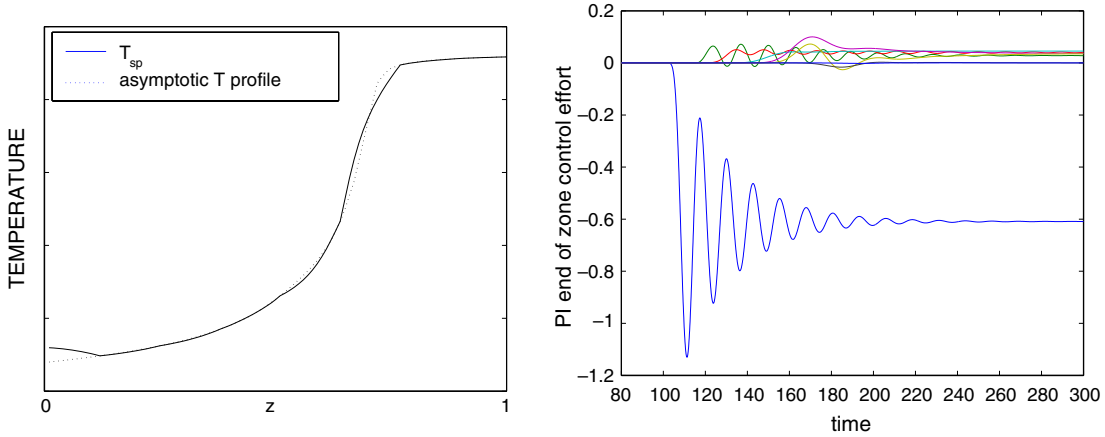

Fig. 5. PI controller with measurement at the end of the zone. Performance of the closed loop system when a step of amplitude 10% of input temperature is applied at the entrance of the reactor. Left: asymptotic temperature profile. Right: control effort.

controller is turned off. Thus for the sake of simplicity, we neglect the integral terms.

Perturbation analysis of disturbance rejection. Consider two adjacent zones $i-1$ and i, we wish to estimate the attenuation of a step disturbance of amplitude d entering at the beginning of zone $i-1$. One can ask where the best location $\alpha \in [0,1]$ for the temperature measurement is for having the highest attenuation onto the next zone. Having $\alpha = 1$ or $\alpha = 0$ means that the measurement is performed at the beginning or at the end of the zone respectively. Once controlled by one of the proposed controllers, the temperature PDE is a transport equation in first order approximation. Assuming that stability is achieved by the previous control loops, perturbation in the control δu affects the temperature by the following integral formula for all $x \in [0,1]$

$$\delta T(i-x,t) = \delta T(i-1, t-(1-x)) + \int_{t-(1-x)}^{t} \tilde{B}(t-s)\delta u_i(s)\,\mathrm{d}s,$$

with $\tilde{B} > 0$. Now assume that δu_i is a closed loop signal $\delta u_i(t) = -K_i T(i-\alpha, t)$. Steady state values satisfy

$$T(i-x,\infty) = \frac{1 + K_i \int_{1-x}^{1-\alpha} \tilde{B}(s)\,\mathrm{d}s}{1 + K_i \int_{0}^{1-\alpha} \tilde{B}(s)\,\mathrm{d}s} T(i-1,\infty)$$

and in particular

$$T(i,\infty) = \frac{1 - K_i \int_{1-\alpha}^{1} \tilde{B}(s)\,\mathrm{d}s}{1 + K_i \int_{0}^{1-\alpha} \tilde{B}(s)\,\mathrm{d}s} d.$$

As K_i increases (strong gains seem often a good option, especially with the Ziegler–Nichols tuning rules), the disturbance is attenuated from the entrance of the zone to the exit by a factor asymptotically equal to

$$-\int_{1-\alpha}^{1} \tilde{B}(s)\,\mathrm{d}s \Big/ \int_{0}^{1-\alpha} \tilde{B}(s)\,\mathrm{d}s.$$

Since $\alpha > 0$, this term is negative. The optimum is to choose $\alpha = 0$, meaning the best measurement location in terms of disturbance rejection is at the end of the zone. With this choice, the disturbance does not propagate to the next zone. If a different choice is made (e.g. centre of the zone measurement), then the disturbance propagates with an opposite sign to the next zone. This explains the steady state reached with the center of the zone measurement in Fig. 4. On the contrary, one can clearly see in Fig. 5 that the disturbance affects mainly the first zone and then is strongly attenuated by the end of the zone measurement controller. Similarly, the control effort is focused on the first zone in Fig. 5.

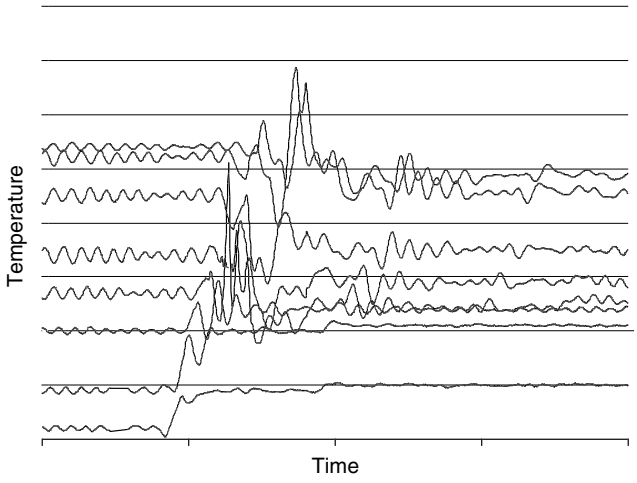

Fig. 6. Industrial results with an end of the zone PI controller (unsatisfactory).

3.4. Industrial results with a PI controller

In Fig. 6, the results of a grade transient are shown. Actual scales are omitted for confidentiality reasons. Yet, it is possible to represent this transient as a non uniform shift in temperature for the different zones ranging from +10% to −5%. The measurement are all performed at the center of the zone except one that is measured at the end. While the regulation is satisfactory before the transient, some oscillations persist. This is mostly due to the high value of the gains chosen for the PI to get a strong hold on the system during transients. The transient itself gives rise to oscillations. In the first zone, the system is steered smoothly by the controller but the next zone is harder to control as the reaction is the strongest. Finally, the last zones are suffering from the disturbances travelling from the first zones. These industrial results are consistent with the study presented in Section 3.1. This behavior was considered a serious bottleneck for the plant productivity and was at the origin of our study on the control upgrade.

4. LQR controller design

In this section, a centralized PI controller is proposed in which the proportional gains are optimally chosen using LQR design. Weights of the input channels are computed through this LQR design. In a future work, we could investigate the use of higher order controller (that may include some explicit or implicit observer for instance). In the sequel, we will refer to this centralized PI scheme as LQR to remind the way the proportional gain was designed.

4.1. Control setup

The LQR is designed to regulate the temperature about the desired profile T_{sp}. To this end, the first

equation of (5) is linearized about $(T_{sp}, x_{sp}, G_{sp}, u_{sp})$. This yields

$$\dot{T} = \left(A + C_p^{-1} \left. \frac{\mathrm{d}r}{\mathrm{d}T} \right|_{(T_{sp}, x_{sp}, G_{sp})} \right) T + Bu. \tag{7}$$

The values of C_p range from 0.4 to 1, and its variation can be roughly seen as a multiplicative disturbance acting on u. We therefore neglect C_p^{-1} multiplying Bu in the control design. As we will explain in a later section, this does not cause a problem due to the robustness properties of the LQR. Define $\overline{A} = (A + C_p^{-1} \left. \frac{\mathrm{d}r}{\mathrm{d}T} \right|_{(T_{sp}, x_{sp}, G_{sp})})$. The LQR problem is solved in each one of the eight zones separately, neglecting the propagation of perturbations from zone i to zone $i+1$. Perturbations are very small in zone $i+1$ if the LQR in zone i is properly designed. This choice is due to numerical issues that arise when considering the problem of assigning the eigenvalues of the relatively large dimensional entire system. Thus, for the control design purpose we have $\overline{A} \cong \mathrm{block-diag}(\overline{A}_1, \ldots, \overline{A}_8)$, with $\overline{A}_1 \in \mathbb{R}^{n_i \times n_i}$ previously defined. Then, we have eight identical LQR problems for the pairs $(\overline{A}_i, B_i)$, with $B_i \in \mathbb{R}^{n_i}$ a vector of ones. For each i the functional

$$J(u) = \int_0^\infty \left(u_i(t)^2 + T_{\sum_{j=1}^{i} n_j}(t)^2 \right) \mathrm{d}t, \tag{8}$$

is minimized, where $T_{\sum_{j=1}^{i} n_j}(t)$ is the temperature at the end of zone i, and $u_i(t)$ is the control input of the same zone. Let $K_{P,i} \in \mathbb{R}^{n_i}$ denote the optimal vector of proportional gains in zone i, we use

$$u_i = -K_{P,i}^{T}(I_p T - T_{sp}) - K_{I,i} \int_0^t (T_{n_i}(s) - T_{sp,i})\, \mathrm{d}s + u_{i,\mathrm{ref}}, \tag{9}$$

where the integral term (tuned a posteriori) guarantees zero asymptotic error with respect to step disturbances at least at the end of the zone. Since we assume to have at most three possible measurements in each zone (i.e. at the beginning which corresponds to the end of the previous zone, at the center, and at the end), we linearly interpolate the measurements we have in each zone in order to do the feedback from the interpolated temperature. The $n_i \times n_i$ matrix I_p models the interpolations, that is $T_{\mathrm{interp}} = I_p T$. Ideally, the larger the number of measurements the closer I_p to the identity matrix.

Fig. 7 reports the behavior of the closed loop system when a step disturbance of 10% is applied at the entrance of the reactor. The left plot shows the asymptotic temperature profile along the reactor. The right plot shows the control effort. Comparisons with Fig. 5 stress that the transients are smoother and the control signal does not oscillate.

4.2. Industrial results with a LQR controller

Fig. 8 shows industrial results obtained with the LQR design that has been in service since 2000 (see [2]). Again, a grade transient is considered, which is different from the one presented in the PI Section but is just as difficult to achieve. Before the transient, the system is well controlled. Residual oscillations are very small compared to the PI results in Fig. 6. This is due to the better suited choice of the gains. The transient itself is satisfactory. It is fast with mostly monotonic trajectories and no propagation of undesirable perturbations between the zones. After the transient, the system is well controlled. This behavior has been considered successful since this new controller was designed and installed. Indirectly, it also allowed to increase the productivity by an upgrade of the total amount of monomer that can be processed (changing the velocity of the flow and reference temperature profiles) without changing any actuators or sensors.

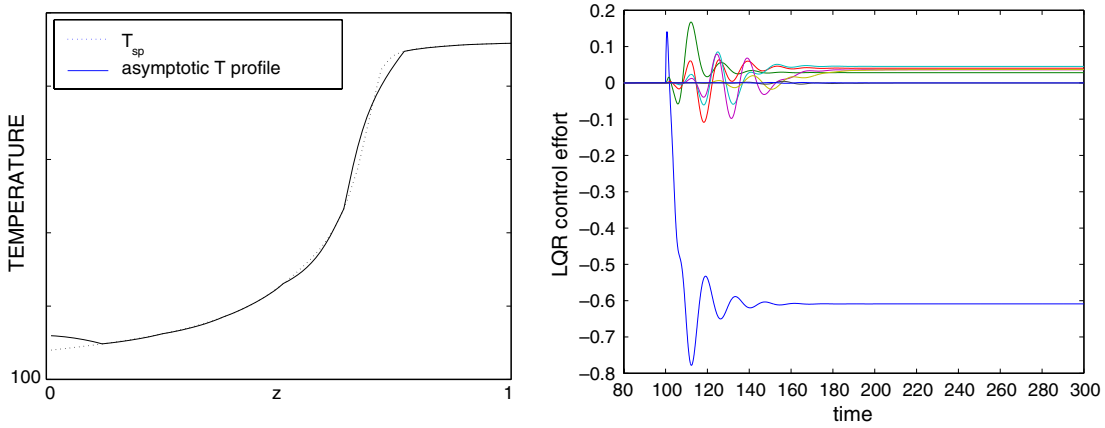

Fig. 7. LQR. Performance of the closed loop system when a step of 10% is applied at the entrance of the reactor.

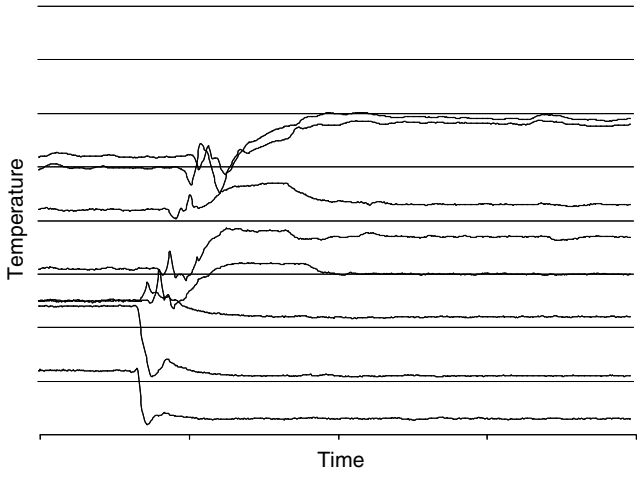

Fig. 8. Industrial results with a LQR controller.

4.3. Comparison between the LQR and the PI with measurement at the end of the zone

The LQR controller is a natural evolution of the decentralized PI control scheme in the case in which a full measurement is possible. It simply provides a methodology for optimally choosing the gains of the proportional controller, and thus it leads to a centralized PI controller structure. A better performance of the LQR controller is to be expected because for designing the proportional gains an optimization is run, and because the number of measurements considered is larger than the one in the decentralized PI scheme. The asymptotic performance of the decentralized PI is comparable to the one of the centralized scheme obtained with LQR design. The transient performance of the LQR design is instead better as expected. To investigate this feature further on, the system was simulated starting from a temperature profile 20% higher than the desired one. The results with the decentralized PI and with the LQR are shown in Fig. 9. The decentralized PI gives rise to instability as its gains were designed around the desired temperature profile. The LQR instead steers the system to the desired profile. This robustness property with respect to unmodelled dynamics is due to the centralized nature of this controller and to the number of measurements. In Fig. 10 (right), the Nyquist plots of $\det[I + H(j\omega)]$ and of $\det[I + \widetilde{H}(j\omega)]$, where $H(s) = K(sI - A)^{-1}B$ and $\widetilde{H}(s) = K(sI - \widetilde{A})^{-1}B$, with $\widetilde{A} = A + BK(I - I_p)$ are depicted. The effect of a poor interpolation is to reduce the robustness margins of the system with respect to input perturbations. In particular, if eight measurements are considered (e.g. only end of the zone sensors are available) the LQR controller results in an unstable closed loop system.

In conclusion, the LQR design turns out to be easy because the exact expression of the kinetics does not need to be known (the x and G dynamics can be neglected), and thus the design considers only the linearized version of the T dynamics. It is more robust than the PI with measurement at the end of the zone, this being due to its centralized structure and to the quality of the measurement interpolation.

5. Nonlinear trajectory generation control approach

In the latest years, optimal control problems with systems governed by partial differential equations subject to control and state constraints have been extensively studied. We refer for instance to [18] for necessary optimality conditions for special cases of elliptic problems and to [19,20] for numerical studies. One may think to use these tools as a closed loop controller as in estab-

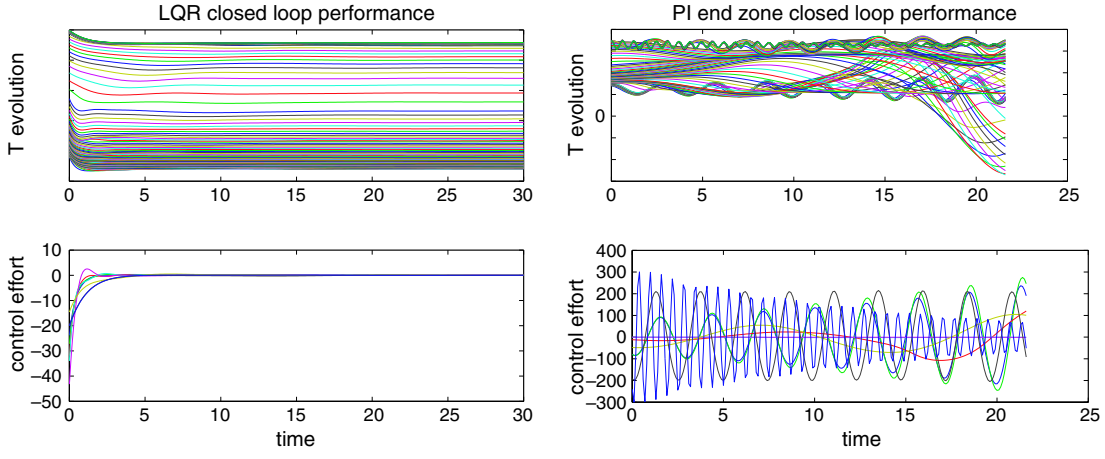

Fig. 9. Performance of the LQR controller with 17 uniformly distributed measurements (left plot) and of the decentralized PI with measurements at the end of the zone (right plot), when the system is started at a temperature profile 20% higher that the desired one T_{sp}.

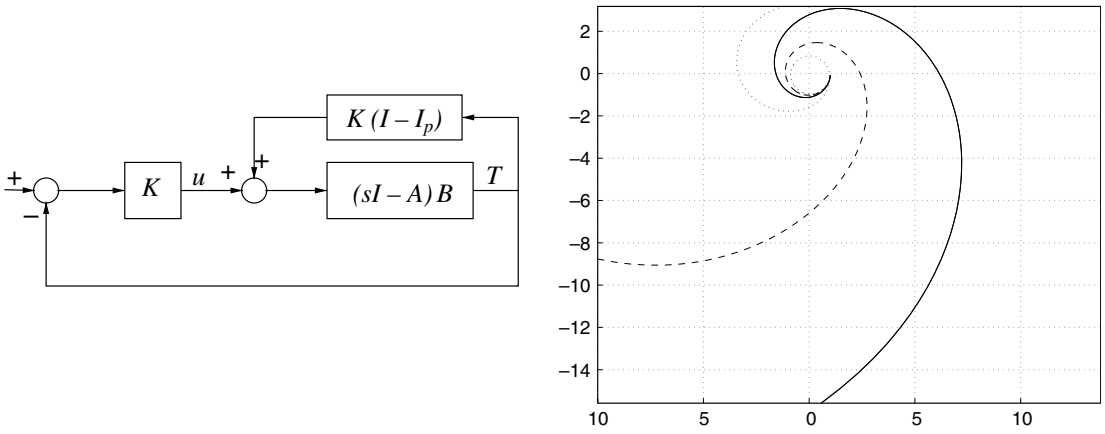

Fig. 10. Linearized temperature control loop (left). Nyquist plot of $\det[I + H(\mathrm{j}\omega)]$ (solid line), and of $\det[I + \widetilde{H}(\mathrm{j}\omega)]$ for two different interpolations. The dashed plot corresponds to a number of 24 uniformly distributed measurements along the reactor, while the dotted plot corresponds to a number of 17 uniformly distributed measurements.

lished receding horizon control strategies for systems governed by ordinary differential equations (see [21,22] for instance).

A direct method to solve these problems is to use finite dimensional approximations for both the control and the state and to enforce constraints at some prescribed grid points (see [23] for an overview of this direct collocation approach). This results in a nonlinear program, see [24,25]. In [6], a different methodology is proposed. For optimal control of nonlinear ordinary differential equations of the form $\dot{x} = f(x) + g(x)u$, where $\mathbb{R} \ni t \mapsto x \in \mathbb{R}^n$ and $\mathbb{R} \ni t \mapsto u \in \mathbb{R}^m$, it is shown [26] that it is possible and computationally efficient to reduce the dimension of the nonlinear programming problem by using inversion to reduce the number of dynamic constraints in the problem. In this approach, variables are eliminated through explicit substitutions. The "inversion" concept can be extended to the field of partial differential equations. For numerical implementation, the variables can be parameterized by tensor-product B-splines (among other basis functions). Their partial derivatives can be easily (analytically) computed, combined, and substituted to as many components of the states and the control as possible in both the cost functions and the constraints.

After the variables have been parameterized in terms of B-spline surfaces, the coefficients $C^l_{i,j}$ of the B-spline basis functions will be found using sequential quadratic programming. This problem is stated as

$$\min_{y \in \mathbb{R}^{N_c}} F(y) \text{ subject to } l_b \leqslant c(y) \leqslant u_b,$$
$$\text{where } y = (C^1_{1,1}, C^1_{1,2}, \ldots, C^p_{p_t,p_x}) \quad \text{and} \quad N_c = p_t * p_x * p. \tag{10}$$

$F(y)$ is the discrete approximation of the chosen objective function. We then use NPSOL [27] as the sequential quadratic programming to solve this new problem.

5.1. Optimal control problem formulation

We consider the variables x and T only, while we neglect the variation of the G value that we assume fixed to its reference G_{sp}. Then we formulate the problem of shifting the temperature profile from a starting profile $T(0,z) = T_{ic}(z)$ to the desired final profile $T(t_{\mathrm{f}},z) = T_{\mathrm{sp}}(z)$ for a given transient time t_{f} as a constrained minimization problem. In this setup we relax the underactuated model by assuming full actuation (we could add constraints on u but this could be expensive in terms of computation time). In particular we want to find the $(t,z) \mapsto (T(t,z),\ x(t,x),\ u(t,z))$ that minimizes the cost

$$J(T,x,u) = \int_{\tau=0}^{t_{\mathrm{f}}} \int_{s=0}^{1} c_1 u(\tau,s)^2 + c_2 (T(\tau,s) - T_{\mathrm{sp}}(s))^2 \,\mathrm{d}\tau\,\mathrm{d}s, \tag{11}$$

subject to the boundary constraints

$$T(0,z) = T_{ic}(z), \quad T(t_{\mathrm{f}},z) = T_{\mathrm{sp}}(z), \quad T(t,0) = T_{\mathrm{inlet}},$$
$$T(0,z) = x_{ic}(z), \quad x(t,0) = x_{\mathrm{inlet}} \tag{12}$$

and to the domain constraints

$$\left(\frac{\partial T(t,z)}{\partial t} + v\frac{\partial T(t,z)}{\partial z}\right) = \frac{r(T,x,G)}{C_p(T,x)} + \frac{u}{C_p(T,x)}, \tag{13}$$

$$\frac{\partial x(t,z)}{\partial t} + v\frac{\partial x(t,z)}{\partial z} = k(T,x,G), \tag{14}$$

$$l_b \leqslant u(t,z) \leqslant u_b. \tag{15}$$

We reduce the number of variables involved in the constrained minimization problem to two, by rewriting u as a function of x and T by means of equation (13). Therefore, the cost in (11) becomes

$$J(T,x) = \int_{\tau=0}^{t_{\mathrm{f}}} \int_{s=0}^{1} c_1 \left(\left(\frac{\partial T(\tau,s)}{\partial \tau} + v\frac{\partial T(\tau,s)}{\partial s}\right) C_p(T,x) - r(T,x,G) \right)^2 + c_2 T(\tau,s)^2 \,\mathrm{d}\tau\,\mathrm{d}s,$$

subject to the boundary constraints given in Eq. (12), and to the domain constraints

$$\frac{\partial x(t,z)}{\partial t} + v\frac{\partial x(t,z)}{\partial z} = k(T,x,G), \tag{16}$$

$$0 \leqslant x(t,z) \leqslant 1 - c_0, \tag{17}$$

$$l_b \leqslant \left(\frac{\partial T(t,z)}{\partial t} + v\frac{\partial T(t,z)}{\partial z}\right) C_p(T,x) - r(T,x,G) \leqslant u_b, \tag{18}$$

where we added the domain constraint on the x values to avoid any sign change for the argument of the square root in the reaction expression given in (4). This term would become negative if this constraint is violated and thus the numerical solver would fail.

Once the optimal solution $T^{\text{opt}}(t,z)$, $x^{\text{opt}}(t,z)$ has been found, the optimal input is computed as

$$u^{\text{opt}}(t,z) = \left(\frac{\partial T^{\text{opt}}(t,z)}{\partial t} + v\frac{\partial T^{\text{opt}}(t,z)}{\partial z}\right) C_p(T^{\text{opt}}, x^{\text{opt}}) - r(T^{\text{opt}}, x^{\text{opt}}, G).$$

5.2. Optimal solutions

The NTG software package [26,6] is used to solve the constrained optimization problem explained in the previous section. Typical problems that can be solved with this package include the example given in Fig. 11 where the parameters are set as $c_1 = c_2 = 1$, $l_b = -20$, $u_b = 20$, constraints are enforced on a 16×16 uniform grid, Eq. (14) is satisfied with a tolerance of 10^{-5}. The total number of spline coefficients is 144. In this problem the initial temperature offset is distributed along the reactor with a peak at 25. The optimal control strategy saturates the constraints.

5.3. Using NTG with a closed loop controller

The optimal control input computed by NTG is then used in our simulator. In addition to the open loop optimal control, we use also a closed loop controller to be able to track the optimal temperature evolution T^{opt}. Let $\mathbf{u}^{\text{opt}}(t) = (u^{\text{opt}}(t,z_1),\ldots,u^{\text{opt}}(t,z_n))^{\text{T}}$, and $\mathbf{T}^{\text{opt}}(t) = (T^{\text{opt}}(t,z_1),\ldots,T^{\text{opt}}(t,z_n))^{\text{T}}$, then the control input $u \in \mathbb{R}^8$ used in model (5) is

$$u(t) = (B^{\text{T}}B)^{(-1)}B^{\text{T}}(\mathbf{u}^{\text{opt}}(t)) - K(I_p T(t) - \mathbf{T}^{\text{opt}}(t)),$$

with K a scalar constant. This last expression takes into account the under-actuated structure of our model by doing a least square approximation of the optimal control value. This strategy addresses the problem of regulation of distributed process with spatially-distributed control actuators and measurement sensors. In NTG the system is treated as a fully distributed system, the feedback term takes care of the imperfections of this

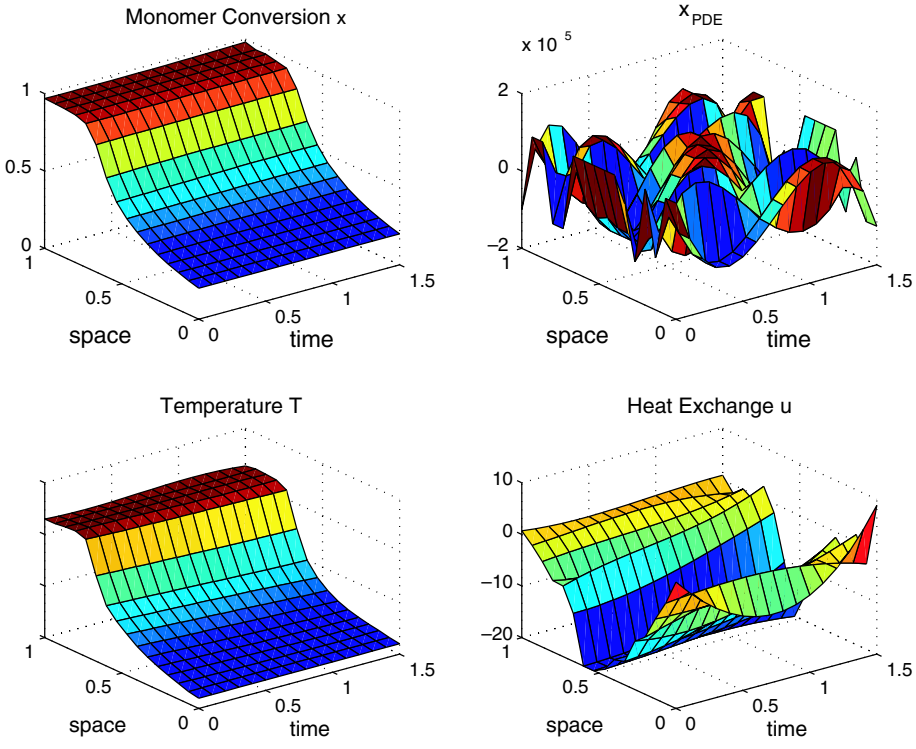

Fig. 11. Optimal solution found by the NTG software. We show the two dimensional plots of the optimal quantities on the grid where the constraints were enforced and the cost was minimized.

model. Further, this feedback term is needed for attenuating numerical and initialization errors in addition to errors due to the G unmodelled dynamics. The linearization about points on the optimal trajectory of the overall system, as this appears in equations (5), gives rise to complex eigenvalues with negative real parts. Even if the system is stable around the optimal trajectory, the presence of a non zero imaginary part gives rise to oscillations when a small error is present, due to the above explained factors. The amplitude of such oscillations become small after a time, which depends on the dynamics of the system, that is larger than the target final time t_f. The feedback term eliminates these oscillations within the final time t_f. As we can see from Fig. 12 the open loop control and the close loop one are very similar, meaning that only a small amount of error needs to be corrected.

Numerical setup. In the cost given in (11), we chose $c_1 = c_2 = 1$. The bounds on the input in (15) have been chosen to be $l_b = -100$, $u_b = 100$. The tolerance on the satisfaction of the x PDE given in (14) was chosen to be 10^{-2}. The two-dimensional t, z plots of the quantities $T^{\mathrm{opt}}(t,z)$, $x^{\mathrm{opt}}(t,z)$, $u^{\mathrm{opt}}(t,z)$ are reported in Fig. 11.

The computational time needed for computing the solutions is 4 minutes when the number of spline

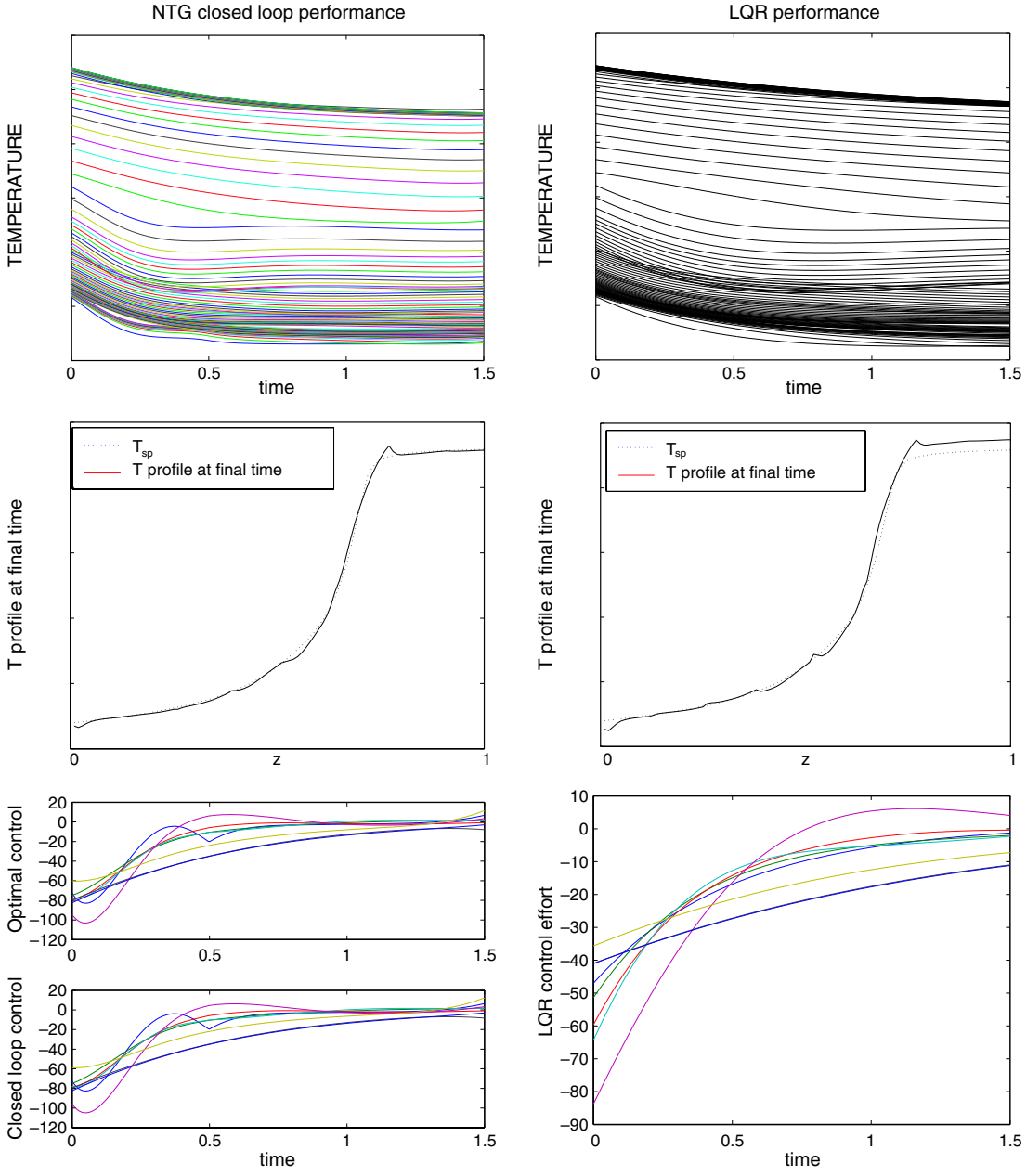

Fig. 12. Performance of the NTG controller (left plots), and of the LQR controller (right plots).

coefficients is 616. The x and T variables are approximated with 6th order B-splines using 6 and 4 knots for the z and t directions respectively. First partial derivatives are continuous across the knots (multiplicity of 2). The constraints are enforced on a 20×10 (z,t) mesh grid. This computation time may seem high when compared to results from the literature (see [28] where SNOPT is used instead of NPSOL) but these refer to systems of parabolic equations. Diffusion terms regularize the solutions of these dynamics and make collocation easier to run thanks to smoothness of the unknown variables. In the problem addressed here, the unknown variables are not very smooth, constraints are thus difficult to enforce and the SQP requires many iterations.

The simulations were run with a fixed step equal to 1.5/300. We show the simulation results in Fig. 12 next to the performance of the LQR designed in the previous section. The values of the cost given in (11) are 1.098×10^3 for the optimal solutions computed by the NTG, it is 1.0978×10^3 for the closed loop quantities obtained from the Simulink simulation, and it is 0.82×10^3 for the LQR. Cost functions are not comparable in this transient mode, but results are of the same order of magnitude. The smaller cost of the LQR is due to a smaller value of the controller, as it appears from Fig. 12, but the behavior of the temperature with the NTG controller is better since it has a faster transient, and it achieves the desired final profile within the target time t_f. This does not happen for the LQR controller whose transient is slower.

5.4. Perspectives of receding horizon control

It is very tempting to use such a numerical tool in the context of receding horizon control (RHC) as detailed in [29,30]. Our control problem incorporates a zero terminal constraint which is consistent with the RHC strategy proposed in [31,32]. One may also use a terminal cost instead, as proposed in [33]. This process has many of the interesting features that make RHC attractive for industrial applications (see [23]): frequent grade changes, possibly large disturbances. Because computational efficiency is vital to the success of such an online optimization, it seems important to test whether our numerical approach can be improved further. One way to achieve shorter computations time is to use well chosen initial guesses. As an example, we investigated the time required to solve the problem given in Fig. 11 with perturbed initial conditions. Results are as follow: the reference solution is computed in 560 s, perturbation of the initial condition offset of 25%, 50% and, 80% are solved using the first run as initial guess in 40, 60 and 80 s respectively (on average). It thus possible to significantly reduce the computational load provided a large enough set of initial guesses is computed offline. In this context, the use of an efficient tool is critical. One could also save more information than just good initial guess. We refer to [34] for a methodology that uses precalculated reference trajectories along with Hessians and gradients information in a real-time embedding strategy. It can also be interesting to consider alternative control configuration to propose a fault tolerant control strategy (as in [35]). This can be done by computing relevant initial guesses for such configurations. More work needs to be done though. A set of costs and terminal constraints has to be well chosen to provide stability in closed loop (see [32] for a discussion on this topic in the case of ordinary differential equations). Robustness is also an issue since computation time cannot be upper bounded (the number of SQP iterations is not limited [23]). It might be interesting to use feasible SQP to be able to exit in a prescribed time with a (possibly suboptimal) feasible solution (see [29] for a discussion on this subject).

6. Conclusion

In this paper, we have shown the main differences between four control schemes for the example of an underactuated exothermic tubular reactor. In particular, we considered a decentralized PI design with two different measurement schemes, and a centralized PI design in which the gains have been computed by means of an LQR design for the problem of regulating the temperature about a desired profile along the reactor. We then considered a nonlinear control scheme, the NTG controller, for the purpose of shifting fast the temperature between desired profiles along the reactor. Our study confirms the industrial results obtained with PI and LQR controllers and gives insight into the experimentally obtained performance. The measurement at the center of the zone scheme performs badly at locations different from the measured ones, while the measurement at the end of the zone scheme allows a good regulation performance everywhere along the reactor. Further, the LQR design allows faster transients than the decentralized PI controller, and its robustness characteristics allow to well reject uncertainties on the initial conditions. This suggests that such a control scheme can be successfully applied to the problem of shifting fast the operating point between temperature profiles along the reactor. This is confirmed by our simulation and industrial results. Finally, we showed how a nonlinear control scheme, the NTG, can be used to impose constraints on the input values and to shift the operating point between different temperature profiles along the reactor within an established time.

In the industrial framework, the key issue we encountered is the compromise between the need for performance and robustness and the model knowledge, availability of measurements, and limited actuation

available for control. This is according to the results of [1] where the authors also highlight that actual implementation of advanced control theory in the polymerization area requires the improvement of measurement and state estimation techniques. To the light of this study, our recommendations are as follows. If only local temperature measurements are available, and one lacks knowledge of the kinetic law, we recommend using the end of the zone measurement scheme. If interpolation of the sensor values is accurate and the knowledge of the kinetics law appears reliable, then we recommend using the LQR for the sake of performance improvement. Finally, if a distributed control system (DCS) is available on site, and if the kinetics law are accurately known, then we suggest that a numerical tool, such as the one presented here, be used. The advantages of using such an approach are: constraints handling, and optimization with respect to the true nonlinear dynamics.

Acknowledgements

We gratefully thank Mr. Creff for his scientific support, Mr. Scarselli, Mr. Germain, Mr. Noel, Mr. de Linares, and Mr. Boueilh from the ATOFINA company for this work and TOTAL for his financial support.

References

[1] M. Embirucu, E.L. Lima, J.C. Pinto, A survey of advanced control of polymerization reactors, Polymer Engineering and Science 36 (4) (1996) 433–447.
[2] N. Petit, Systèmes à retards, platitude en génie des procédés et contrôle de certaines équations des ondes, Ph.D. thesis, Ecole des Mines de Paris, 2000.
[3] T. Larsson, S. Skogestad, Plantwide control—a review and new design procedure, Modeling Identification and Control 21 (4) (2000) 209–240.
[4] H. Cui, E.W. Jacobsen, Performance limitations in decentralized control, Journal of Process Control 12 (4) (2002) 485–494.
[5] W. Wang, D.E. Rivera, K.G. Kempf, Comparison of centralized versus decentralized model predictive control strategies to semiconductor manufacturing supply network, in: Proceedings of the 2003 American Control Conference, 2003.
[6] N. Petit, M.B. Milam, R.M. Murray, A new computational method for optimal control of a class of constrained systems governed by partial differential equations, in: Proceedings of the 15th IFAC World Congress, 2002.
[7] R.M. Murray, J. Hauser, A. Jadbabaie, M.B. Milam, N. Petit, W.B. Dunbar, R. Franz, Online control customization via optimization-based control, in: G. Balas, T. Samad (Eds.), Software-enabled Control, Information Technology for Dynamical Systems, Wiley-Interscience, 2003, pp. 149–174.
[8] M.P. Vega, E.L. Lima, J.C. Pinto, Modeling and control of tubular solution polymerization reactors, Computers and Chemical Engineering 21 (13) (1997) 1049–1054.
[9] C. Antoniades, P.D. Christofides, Integrating nonlinear output feedback control and optimal actuator/sensor placement for transport-reaction processes, Chemical Engineering Science 56 (2001) 4517–4535.
[10] A.W.T. Hui, A.E. Hamielec, Thermal polymerization of styrene at high conversion and temperatures. an experimental study, Journal of Applied Polymer Science 16 (1972) 749–769.
[11] G. Odian, Principles of Polymerization, third ed., John Wiley & Sons, 1991.
[12] O. Levenspiel, Chemical Reaction Engineering, third ed., John Wiley & Sons, Inc., 1999.
[13] D.M. Bošković, M. Krstić, Backstepping control of chemical tubular reactors, Computers and Chemical Engineering 26 (7–8) (2002) 1077–1085.
[14] E.F. Costa Jr., P.L.C. Lage, E.C. Biscaia Jr., On the numerical solution and optimization of styrene polymerization in tubular reactors, Computers and Chemical Engineering 28 (1–2) (2004) 27–35.
[15] R. Dautray, J.-L. LionsMathematical Analysis and Numerical Methods for Science and Technology, vol. 6, Springer-Verlag, 1993.
[16] M. Morari, E. Zafiriou, Robust Process Control, Prentice-Hall, Englewood Cliffs, 1989.
[17] K. Astrom, T. Hagglund, PID Controllers: Theory, Design, and Tuning, second ed., ISA—The Instrumentation, Systems, and Automation Society, 1995.
[18] J.-L. Lions, Optimal Control of Systems Governed by Partial Differential Equations, Springer-Verlag, 1971.
[19] H. Maurer, H. Mittelmann, Optimization techniques for solving elliptic control problems with control and state constraints. Part 2: Distributed control, Computational Optimization and Applications 18 (2001) 141–160.
[20] L.T. Biegler, O. Ghattas, M. Heinkenschloss, B. van Bloemen Waanders, Large-scale PDE-constrained optimization, Lecture Notes in Computational Science and Engineering, vol. 30, Springer Verlag, 2003.
[21] S.J. Qin, T. Badgwell, A survey of industrial model predictive control technology, Control Engineering Practice 11 (2003) 733–764.
[22] J.B. Rawlings, Tutorial overview of model predictive control, IEEE Control Systems Magazine (2000) 38–52.
[23] T. Binder, L. Blank, H.G. Bock, R. Bulirsch, W. Dahmen, M. Diehl, T. Kronseder, W. Marquardt, J.P. Schlöder, O. von Stryk, Introduction to model based optimization of chemical processes on moving horizons, in: M. Grötschel, S.O. Krumke, J. Rambau (Eds.), Online Optimization of Large Scale Systems: State of the Art, Springer, 2001, pp. 295–340.
[24] O. von Stryk, R. Bulirsch, Direct and indirect methods for trajectory optimization, Annals of Operations Research 37 (1992) 357–373.
[25] L.T. Biegler, Efficient solution of dynamic optimization and NMPC problems, in: F. Allgöwer, A. Zheng (Eds.), Nonlinear Model Predictive Control, Birkhäuser, 2000, pp. 219–245.
[26] M.B. Milam, K. Mushambi, R.M. Murray, A new computational approach to real-time trajectory generation for constrained mechanical systems, in: IEEE Conference on Decision and Control, 2000.
[27] P.E. Gill, W. Murray, M.A. Saunders, M.A. Wright, User's guide for NPSOL 5.0: a Fortran package for nonlinear programming, Systems Optimization Laboratory, Stanford University, Stanford, CA 94305, 1998.
[28] L. Petzold, J.B. Rosen, P.E. Gill, L.O. Jay, K. Park, Numerical optimal control of parabolic PDEs using DASOPT, in: M. Grötschel, S.O. Krumke, J. Rambau (Eds.), Large Scale Optimization with Applications, Part II, vol. 93, Springer, 1997, pp. 271–300.
[29] F. Allgöwer, T.A. Badgwell, J.S. Qin, J.B. Rawlings, S.J. Wright, Nonlinear predictive control and moving horizon estimation—an introductory overview, in: P.M. Frank (Ed.), Advances in Control, Highlights of ECC'99, Springer, 1999, pp. 391–449.

[30] F. Allgöwer, A. Zheng, Nonlinear predictive control, in: Progress un Systems Theory, vol. 26, Birkhäuser, 2000.
[31] D.Q. Mayne, H. Michalska, Receding horizon control of nonlinear systems, IEEE Transactions on Automatic Control 35 (7) (1990) 814–824.
[32] D.Q. Mayne, J.B. Rawlings, C.V. Rao, P.O.M. Scokaert, Constrained model predictive control: stability and optimality, Automatica 36 (2000) 789–814.
[33] A. Jadbabaie, J. Hauser, On the stability of unconstrained receding horizon control with a general terminal cost, in: Proceedings of the 40th IEEE Conference on Decision and Control, 2001.
[34] M. Diehl, H.G. Bock, J.P. Schlöder, R. Findeisen, Z. Nagy, F. Allgöwer, Real-time optimization and nonlinear model predictive control of processes governed by differential–algebraic equations, Journal of Process Control 12 (2002) 577–585.
[35] N.H. El-Farra, P.D. Christofides, Coordinating feedback and switching for control of spatially distributed processes, Computers and Chemical Engineering 28 (2004) 111–128.